



This is the accepted manuscript made available via CHORUS, the article has been published as:

# First-Principles Prediction of the Equilibrium Shape of Nanoparticles Under Realistic Electrochemical Conditions

Nicéphore Bonnet and Nicola Marzari

Phys. Rev. Lett. **110**, 086104 — Published 20 February 2013

DOI: [10.1103/PhysRevLett.110.086104](https://doi.org/10.1103/PhysRevLett.110.086104)



site on (100), and relaxing the topmost metal layer. The PBE exchange-correlation functional [22] is used, in combination with ultrasoft pseudopotentials for the ion cores [23]. We use a plane-wave cutoff of 30 Ry, a  $7 \times 7 \times 1$  k-point mesh with 0.01 Ry of cold smearing [24] for converged Brillouin zone sampling.

The electrode potential is controlled by adding explicit charges on the slab [12, 18], and a corrective potential is applied, as discussed in [25], to remove undesired periodic-image interactions. The electrochemical double layer is modeled by placing a planar counter-charge at a distance of 3 Å from the metal surface. The dipolar response of water is rendered by inserting a continuum dielectric medium inside the double layer [26]. Cyclic voltammetry and impedance spectroscopy measurements in 0.1-1 M electrolytes have yielded a double layer capacitance  $c_{dl}$  in the range 20-100  $\mu\text{F}/\text{cm}^2$  [27]. Here, a representative value of 40  $\mu\text{F}/\text{cm}^2$  is chosen, which, for the geometry considered, implies a relative permittivity of 13.6, consistent with a previous estimate from MD simulations [28]. Finally, the absolute electrode potential  $\Phi$  is computed as  $-v(\infty) - \epsilon_F/e$ , where  $v(\infty)$  is the value of the electrostatic potential in the flat region outside the double layer, and  $\epsilon_F$  is the Fermi energy. Since this model ignores the chemical effects of water, and in particular its contribution to the surface dipole, the potential of zero charge (PZC) is taken from experimental measures. The CO-charge displacement method gives  $\Phi_{\text{PZC}} \simeq 0.23$  V/SHE [29], where the standard hydrogen electrode (SHE) is by definition a reversible hydrogen electrode in which the pH is set to 0. Other measurements by impedance spectroscopy suggest  $\Phi_{\text{PZC}} \simeq 0.34$  V/SHE [27]. Incidentally, those values happen to be very close to the onset of hydrogen adsorption in acidic medium. Therefore, in this study, the metal surface at 0.3 V/RHE in acidic medium (pH = 0) is treated as neutral. The influence of pH is captured through its entropic effects on the value of the absolute potential of the reversible hydrogen electrode, and consequently on the surface charge of RHE. Thus, at room temperature

$$\Phi_{\text{RHE}} = \Phi_{\text{SHE}} + \frac{kT}{e} \ln[\text{H}^+] \simeq \Phi_{\text{SHE}} - 0.059 \times \text{pH} \text{ (V)}$$

Consequently, the metal surface with the same relative potential of 0.3 V/RHE now bears a non-zero charge density

$$\sigma = -0.059 \times c_{dl} \times \text{pH} \quad (4)$$

Using this electrochemical model,  $\Delta G(\theta)$  is calculated in acidic (pH = 1) and alkaline (pH = 13) conditions (Fig. 1). Interestingly, changing the pH has almost no effect on adsorption energies on Pt(100), while a sizeable effect is observed on Pt(111). To understand the difference, we plot the electrode absolute potential as a function of hydrogen coverage for Pt(100). The results for Pt(100)

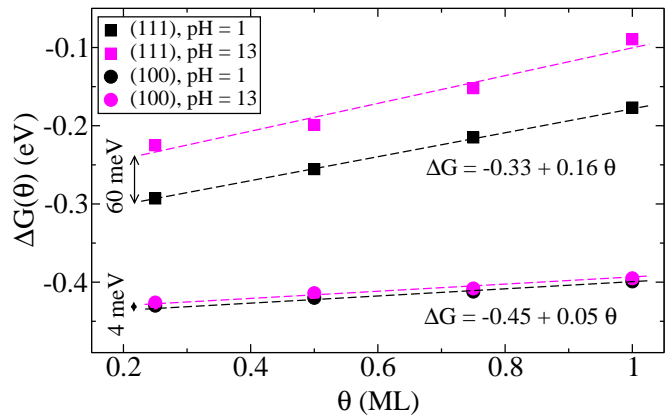


FIG. 1: (Color online) Free energy of the  $\frac{1}{2}\text{H}_2(\text{g}) \rightarrow \text{H}^*$  reaction on Pt(111) and Pt(100) for pH = 1 and pH = 13, along with linear fits. The configurational entropy on the surface is not included.

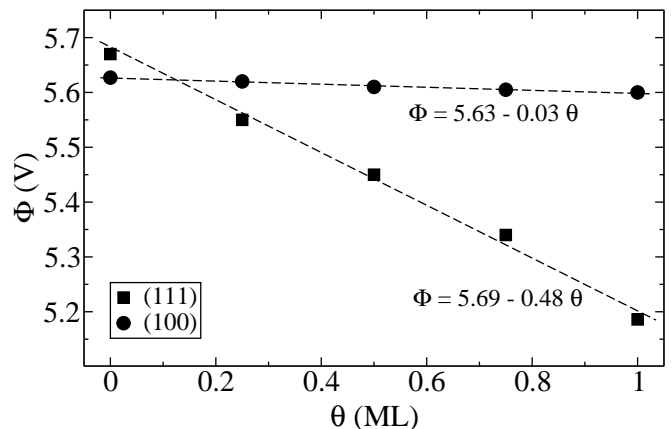


FIG. 2: Electrode absolute potential vs. hydrogen surface coverage for Pt(111) and Pt(100), along with linear fits.

show almost zero slope, suggesting that hydrogen atoms adsorbed on this surface induce only a small change in the surface dipole. By contrast, adsorption of one monolayer of electropositive hydrogen on Pt(111) lowers the potential by about 0.5 V. We attribute this difference to the more dense packing of the (111) surface, contributing to create more sharply defined planes of “negative” Pt atoms and “positive” H atoms. The link between adsorption energy and surface dipole can be formalized by deriving the adsorbate chemical potential  $\mu_H$  from the surface free energy. Considering a surface with  $N$  hydrogen adsorbates and  $q$  free charges, its free energy is

$$G(N, q) = G(N, 0) + \int_0^q \frac{\partial G}{\partial q'} dq' = G(N, 0) + \int_0^q \Phi dq'$$

Taking the derivative with respect to  $N$  to obtain the

chemical potential

$$\mu_H = \frac{\partial G}{\partial N}(N, 0) + \int_0^q \frac{\partial \Phi}{\partial N} dq'$$

or, rewriting in terms of the coverage  $\theta$  and the surface charge density  $\sigma$ , gives

$$\mu_H = \mu_{H,zc} + \frac{1}{\alpha} \int_0^\sigma \frac{\partial \Phi}{\partial \theta} d\sigma',$$

where  $\alpha$  denotes the surface atomic density and  $\mu_{H,zc}$  is the chemical potential on the neutral surface. If, like here,  $\Phi$  varies linearly with  $\theta$ , it leads to the compact expression

$$\mu_H = \mu_{H,zc} + \frac{\sigma \Delta \chi}{\alpha},$$

where  $\Delta \chi$  is the surface dipole change for a full monolayer of hydrogen (-0.03 on (100), -0.48 on (111)). Using Eq. (4) for  $\sigma$ , the chemical potential change upon variation of pH is finally given by

$$\Delta \mu_H = -0.059 \times \frac{c_{dl} \Delta \text{pH} \Delta \chi}{\alpha}.$$

This result confirms that the pH dependence of the adsorption energy is directly proportional to the surface dipole induced by adsorbates. Moreover, this effect can be related to the concept of electrosorption valency. The electrosorption valency  $\lambda$  of the proton can be obtained as the number of electrons transferred to the electrode from the external circuit upon adsorption of one proton at constant potential [30]. This is equal to 1 plus a corrective quantity to compensate for the induced change in the surface potential. Adsorption of one proton on a unit surface area perturbs the potential by  $\delta \Phi = \frac{\Delta \chi}{\alpha}$ , which is compensated by adding  $\eta = \frac{c_{dl} \Delta \chi}{\alpha e}$  electrons to the surface. Consequently, for the chosen value of the capacitance, we have that on Pt(111)  $\lambda = 1 + \eta = 0.91$ , and on Pt(100)  $\lambda = 0.98$ .

Within the under-potential deposition region ( $U = 0-0.5$  V/RHE), the hydrogen surface coverage at equilibrium is obtained by setting  $\Delta G_{\text{tot}} = 0$  in Eq. (3) (Figs. 3 and 4). On Pt(111), experimental coverages obtained from integration of voltammetric currents are included for comparison. On Pt(100), integration of the voltammetric current in alkaline conditions is difficult as it overlaps with the current from OH formation. Therefore, the potential of peak current is used to infer the position of the deposition curve, and it appears to be very close to the curve in acidic conditions. The potential at the onset of electrosorption is related to the low-coverage adsorption energy and appears to be well predicted by the PBE exchange-correlation functional. On the other hand, the slope of the deposition curve is related to H-H lateral interactions on the surface, and they are slightly underestimated on the Pt(111) surface. Of interest is to note

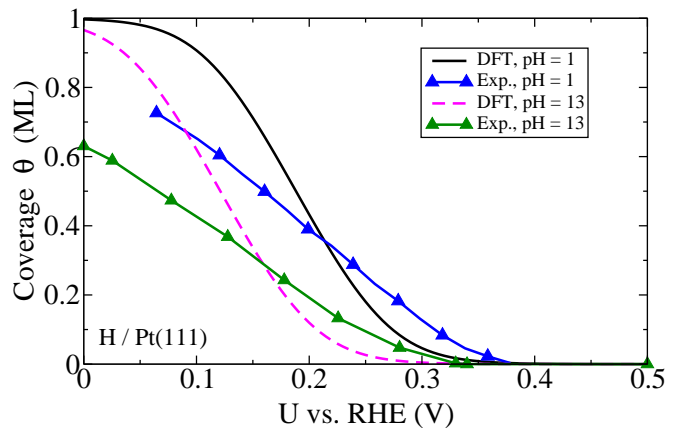


FIG. 3: (Color online) Hydrogen deposition on Pt(111) in the low potential region for acidic and alkaline conditions. Experimental data are from [31, 32].

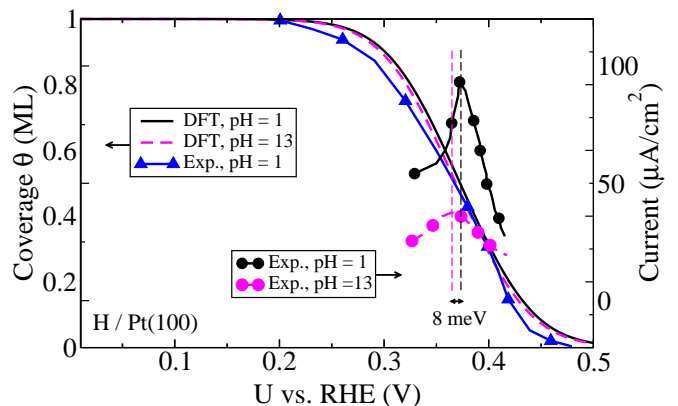


FIG. 4: (Color online) Hydrogen deposition on Pt(100) in the low potential region for acidic and alkaline conditions. Integration of the experimental current in KOH electrolyte (pH = 13) is hindered by overlap with the OH discharge current. The position of the electrosorption curve is then inferred from the potential of peak voltammetric current, which is very close to the value of the same quantity in acidic medium. Experimental data are from [31, 32].

the shift of the (111) curve towards lower potentials for higher pH, a direct consequence of the surface dipole effect discussed earlier.

The potential dependence of the surface energy  $\gamma$  in the presence of electrosorbed species can be expressed by the electrocapillary equation [33]

$$d\gamma = \lambda \theta \alpha e dU.$$

In other words, the surface energy can be directly obtained by integrating  $\theta$  as a function of  $U$  from high to low potentials (Fig. 5). The starting point, i.e. the surface energy of the bare facet, is taken from [34], where the following values are computed with the same formalism used here:  $\gamma_{111} = 1.49$  J/m<sup>2</sup> and  $\gamma_{100} = 1.81$  J/m<sup>2</sup>. In

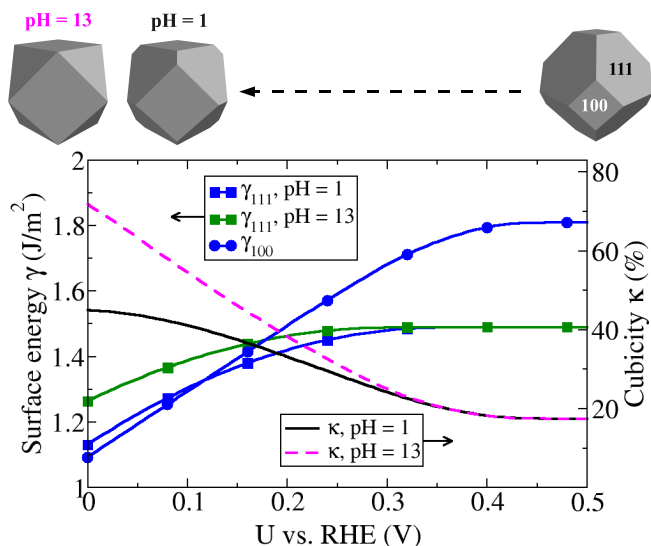


FIG. 5: (Color online) Pt(111) and Pt(100) surface energies as obtained from application of the electrocapillary equation to the hydrogen deposition curves for different pHs, and changes in the nanoparticle shape, as a function of applied potential.

a simplified model where a Pt nanoparticle would only consist of (111) and (100) facets, as suggested by experimental and computational studies [35], the energy-minimizing shape can be found by applying the Wulff construction [36]. In this case, a degree of “cubicity”  $\kappa$  can be defined as the ratio of (100) facets over the total nanoparticle surface area, that depends only on the surface energy ratio  $\frac{\gamma_{111}}{\gamma_{100}}$ . As the electrode potential is scanned to lower potentials, hydrogen deposition occurs earlier on Pt(100) due to a higher reactivity, leading to a greater stabilization of the surface compared to Pt(111). As a consequence, the equilibrium nanoparticle shape becomes more cubic. In alkaline conditions, that effect is reinforced by the reduced hydrogen binding on Pt(111). The octahedric-to-cubic thermodynamic transition, here quantified for stable Pt nanoparticles, is a phenomenon observed experimentally in slightly different circumstances: it has been shown that hydrogen permeating from the anode to the cathode of a proton exchange membrane fuel cell can reduce Pt ions present in solution and produce nanoparticles having a more pronounced cubic aspect as the hydrogen concentration becomes larger [37].

In summary, we here provide an approach to calculate surface energies and equilibrium shapes of nanoparticles for realistic electrochemical conditions and applied potentials. In the process, we determine surface energies as a function of coverage, chemical potentials as a function of pH, and electroadsorption valencies from first-principles. We apply this to the study of hydrogen electrodeposition on Pt surfaces, showing how pH indirectly affects ad-

sorbate energies through the surface charge of the RHE interacting with the surface dipole induced by the adsorbates. Derivation of surface energies from electroadsorption curves, via the electrocapillary equation, leads to the determination of nanoparticles’ equilibrium shapes and shows the ability of the formalism to relate the key factors determining catalytic activity, namely electric bias, electrolyte pH, adsorbate coverage, surface stability and catalyst geometry.

We are grateful to Y. Shao-Horn for valuable discussions. This work was supported primarily by the MRSEC Program of the National Science Foundation under award number DMR - 0819762.

- [1] M. Pourbaix, *Corr. Sc.* **14**, 25 (1974).
- [2] H.A. Gasteiger, S.S. Kocha, B. Sompalli and F.T. Wagner, *Appl. Catal. B: Environ.* **56**, 9 (2005).
- [3] H.A. Gasteiger and N.M. Marković, *Science* **324**, 48 (2009).
- [4] J.K. Nørskov, M. Scheffler and H. Toulhoat, *MRS Bulletin* **31**, 669 (2006).
- [5] B. Hammer and J.K. Nørskov, *Nature* **376**, 238 (1995).
- [6] K. Reuter, D. Frenkel and M. Scheffler, *Phys. Rev. Lett.* **93**, 116105 (2004).
- [7] J.K. Nørskov, J. Rossmeisl, A. Logadottir, L. Lindqvist, J.R. Kitchin, T. Bligaard and H. Jónsson, *J. Phys. Chem. B* **108**, 17886 (2004).
- [8] N.M. Marković and P.N. Ross, *Surf. Sc. Rep.* **45**, 117 (2002).
- [9] B. Hammer and J. K. Nørskov, *Adv. Catal.* **45**, 71 (2000).
- [10] J.K. Nørskov, F. Abild-Pedersen, F. Studt and T. Bligaard, *PNAS* **108**, 937 (2011).
- [11] V.R. Stamenkovic, B. Fowler, B.S. Mun, G. Wang, P.N. Ross, C.A. Lucas and N.M. Marković, *Science* **315**, 493 (2007).
- [12] C.D. Taylor, S.A. Wasileski, J.-S. Filhol and M. Neurock, *Phys. Rev. B* **73**, 165402 (2006).
- [13] A.Y. Lozovoi and A. Alavi, *Phys. Rev. B* **68**, 245416 (2003).
- [14] J. Rossmeisl, E. Skúlason, M.E. Björketun, V. Tripkovic and J.K. Nørskov, *Chem. Phys. Lett.* **466**, 68 (2008).
- [15] M. Otani and O. Sugino, *Phys. Rev. B* **73**, 115407 (2006).
- [16] C. Stoffelsma, P. Rodriguez, G. Garcia, N. Garcia-Araez, D. Strmcnik, N.M. Marković and M.T.M. Koper, *J. Am. Chem. Soc.* **132**, 16127 (2010).
- [17] J. Cheng and M. Sprik, *Phys. Rev. B* **82**, 081406 (2010).
- [18] I. Dabo, N. Bonnet, Y. L. Li and N. Marzari, “Fuel cell science : theory, fundamentals, and biocatalysis” edited by A. Wieckowski and J. Nørskov, Wiley, 2010, Chap. 13.
- [19] G.S. Karlberg, T.F. Jaramillo, E. Skúlason, J. Rossmeisl, T. Bligaard and J.K. Nørskov, *Phys. Rev. Lett.* **99**, 126101 (2007).
- [20] CRC Handbook of Chemistry and Physics, CRC press, 84<sup>th</sup> ed., 2003-2004, p. 5-76.
- [21] P. Giannozzi et al., *J. Phys.: Condens. Matter* **21**, 395502 (2009); <http://www.quantum-espresso.org>.
- [22] J.P. Perdew, K. Burke and M. Ernzerhof, *Phys. Rev. Lett.* **77**, 3865 (1996).

- [23] D. Vanderbilt, Phys. Rev. B **41**, 7892 (1990).
- [24] N. Marzari, D. Vanderbilt, A. De Vita and M.C. Payne, Phys. Rev. Lett. **82**, 3296 (1999).
- [25] I. Dabo, B. Kozinsky, N.E. Singh-Miller, N. Marzari, Phys. Rev. B **77**, 115139 (2008).
- [26] D.A. Scherlis, J.-L. Fattebert, F. Gygi, M. Cococcioni and N. Marzari, J. Chem. Phys. **124**, 074103 (2006).
- [27] T. Pajkossy and D.M. Kolb, Electrochim. Act. **46**, 3063 (2001).
- [28] M. Otani, I. Hamada, O. Sugino, Y. Morikawa, Y. Okamoto and T. Ikeshoji, J. Phys. Soc. Jap. **77**, 024802 (2008).
- [29] A. Cuesta, Surf. Sc. **572**, 11 (2004).
- [30] R. Jinnouchi, T. Hatanaka, Y. Morimoto and M. Osawa, Phys. Chem. Chem. Phys. **14**, 3208 (2012).
- [31] N.M. Marković, B.N. Grgur and P.N. Ross, J. Phys. Chem. B **101**, 5405 (1997).
- [32] N.M. Marković, H.A. Gasteiger and P.N. Ross, J. Phys. Chem. **100**, 6715 (1996).
- [33] P. Delahay, "Double layer and electrode kinetics", Wiley, 1965, Chap. 2.
- [34] N.E. Singh-Miller and N. Marzari, Phys. Rev. B **80**, 235407 (2009).
- [35] A.S. Barnard and L.Y. Chang, ACS Catal. **1**, 76 (2011).
- [36] G. Wulff, Z. Kristallogr. Mineral. **34**, 449 (1901).
- [37] J. Ferreira and Y. Shao-Horn, Electrochem. Solid-St. Lett. **10**, B60 (2007).